Experimental Studies of the Losses and Radiations Due to Bends in the Goubau Line

JIRO CHIBA, MEMBER, IEEE

Abstract—**The losses due to the bending of the Goubau line (*G* line) are determined by experiments. The losses are measured for wide ranges of radius of curvature, bending angle, and the transmission frequency. These three variables determine the losses. It is believed that radiation from a surface-wave transmission line system occurs mainly from the bends and horn in the transmission line system. Directional patterns of such radiation were obtained from measurements.**

I. Introduction

THE emission of electromagnetic waves at a band in the *G* line will cause transmission loss, electromagnetic wave disturbance, signal distortion, and other undesirable effects.

Takiyama [1] explained the losses at the bent section by the analytical four-terminal network method. Suzuki [2] calculated theoretically the losses at the bent section with an ingenious mathematical technique. Suzuki and Inezu [3], Moriwaki and Kawamura [4], Yasaku [5], and Goubau and Sharp [6] reported experimental values. In this paper we introduce a bending angle θ and radius of curvature ρ defined in Fig. 1. Suzuki succeeded in the calculation by assuming that there is only the bending angle (without consideration of radius of curvature ρ). The actual *G* line has a radius of curvature so that this approach is not accurate enough for design analysis and calculation. Previous experimental reports do not extend to wide enough ranges of the three variables, ρ, θ, and frequency f.

The Uchida and Nishida [7] paper considers the ρ and matches very well with experimental values under the limitation of small values of θ. Their conclusions do not agree with experimental values for large θ.

In view of the preceding circumstances, we made experimental measurements, with wide variations in ρ, θ, and f, for the losses at the bent section of the *G* line. Section III evaluates the horizontal patterns of radiation from bends in the transmission line at various angles and with various radii of curvature. Horizontal patterns of radiation from the launching horn were also measured.

II. Measurement of Losses at the Bent Section

A. Detailed Explanation on the Experimental Setup

The experimental setup on the flat field is shown in Figs. 1 and 2. The *G* line is located 5 m above the ground. The sending horn is connected to the admittance bridge by means of the three-stub tuner as shown in Figs. 1 and 2.

Manuscript received January 17, 1975; revised May 25, 1976.
The author is with the Department of Electrical Engineering, Tohoku University, Aoba Aramaki, Sendai, Japan.

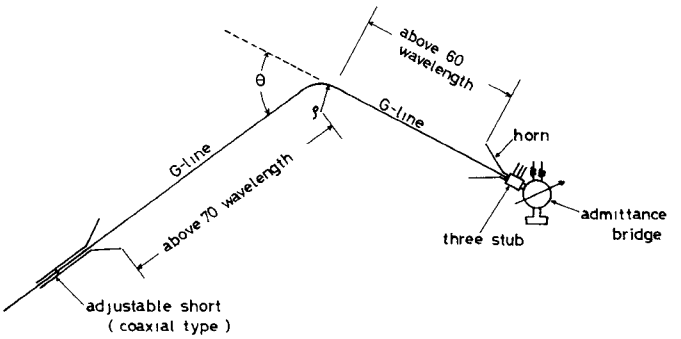

Fig. 1. Experimental setup.

The losses and the radiations due to the bending of the *G* line will change for different values of θ, ρ, and f. The bending angles were marked on the ground as shown in Fig. 3 to indicate the θ clearly and accurately for the measurements. The ρ were fixed by gauges (circular plate and ring) of radii 2.5, 25, and 50 cm, so that the same bending radii can be reproduced for the different tests.

The line tested is described as "4/12 *G* line" and consisted of hard copper of 4-mm diameter, polyethylene insulated with an outside diameter of 12 mm. The line was supported with nylon fishing strings to hold the right bending radius, as shown in Fig. 2.

B. Measurement and Calibration Schemes

Measurement: The Deschamps–Storer method was used to measure the losses. The losses due to bending were obtained by subtracting the measured values for a straight *G* line from the values for the same bent *G* line. The scattering matrix was obtained by plotting the input admittance of the transmission line on the Smith chart.

The intrinsic insertion loss α is given by

$$= -10 \log_{10} \frac{|S_{12}|^2}{1 - |S_{11}|^2} \text{ dB} \qquad (1)$$

where S_{12} and S_{11} are the penetration and reflection constants, respectively, for the matrix elements.

Calibration: It is well known that the Deschamps–Storer method is simple in measurement and experimental error is less. In order to confirm this fact on the present experimental setup, we made calibrations by using a known standard sample of the transmission line. We used the straight *G* line as a standard sample of the transmission losses, because we can calculate the exact transmission

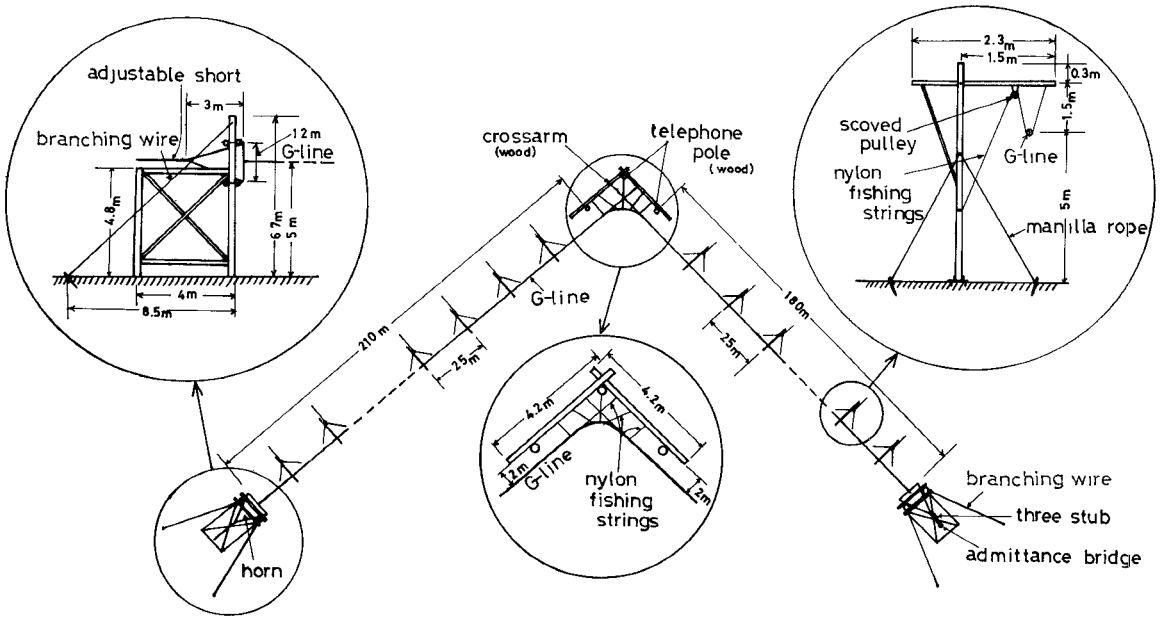

Fig. 2. Experimental setup.

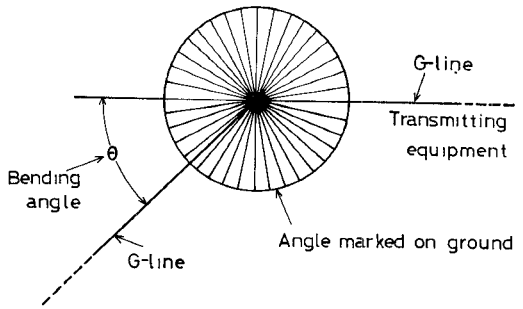

Fig. 3. Determination of θ.

losses of the straight G line according to the equation derived by Goubau.

The experimental values of the losses of the straight G line agree well with the detailed calculation results, the relative error being less than 0.7 percent.

Purity of the Surface-Wave Mode: Existence of the surface-wave mode can be confirmed easily by comparison of the experimental results of the field distribution with calculated results of the field distribution.

C. The Experimental Results of the Losses Due to Bends

The results of the experimentation are shown in Figs. 4–6 from Fig. 4. The experimental results may be summarized as follows.

1) The losses due to bending are seen to be proportional to the θ^2 (for small angles).

2) The rate of increasing loss is much less than the ratio of increased bending angle when the angle is larger than 45°.

3) The change of losses with ρ are relatively small compared to the change of losses with θ when the values of θ and f are small.

The relation between loss and radius of curvature is

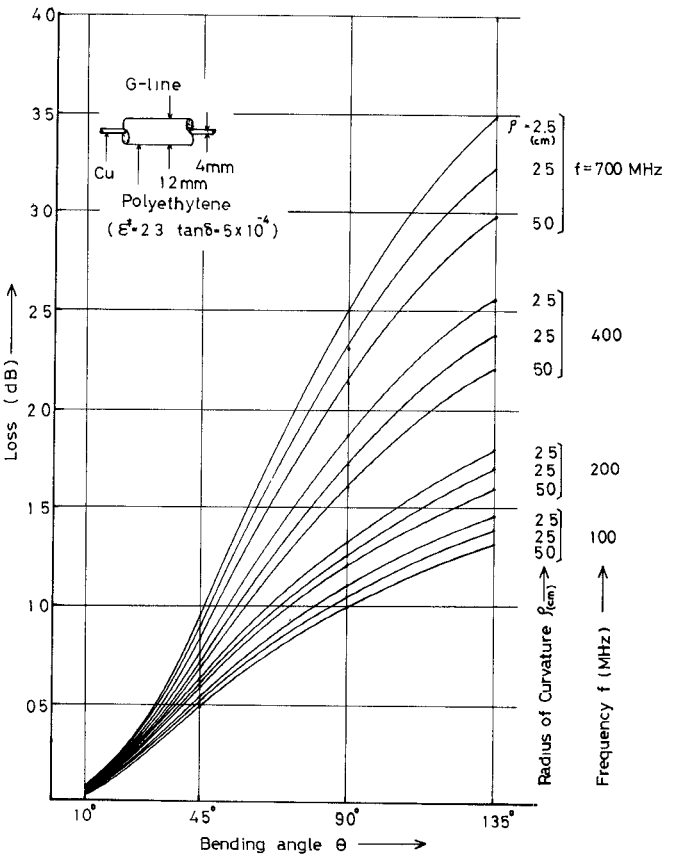

Fig. 4. Loss due to bends.

shown in Fig. 5 (based on Fig. 4). The change of losses with frequency based on Fig. 4 is shown in Fig. 6.

For a low-loss transmission line it is desirable to divide a large bending angle θ into several small bending angles.

The velocity increases towards the outer side of the curved transmission line because, as is evident from

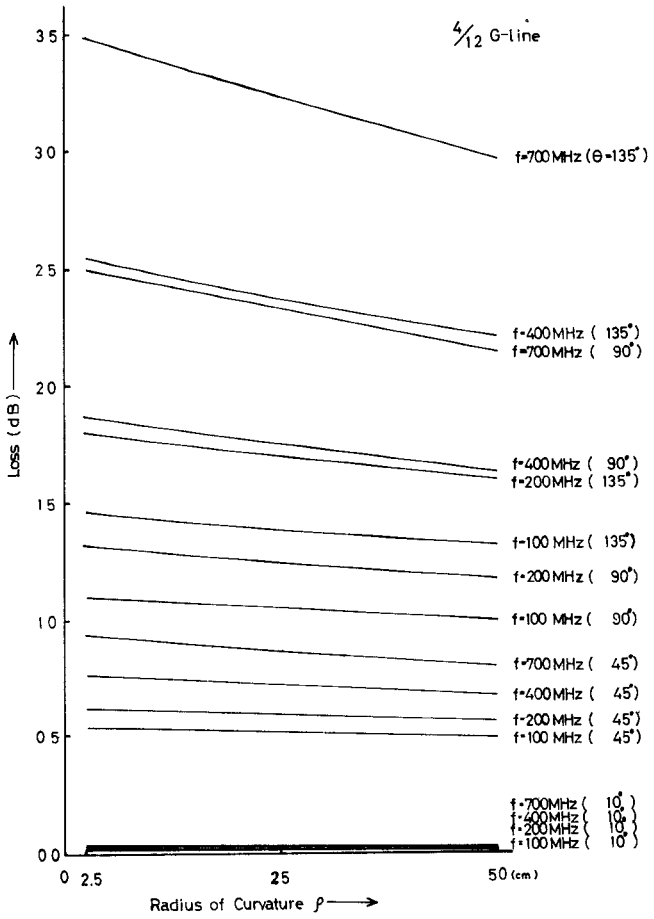

Fig. 5. Relation between loss and radius of curvature.

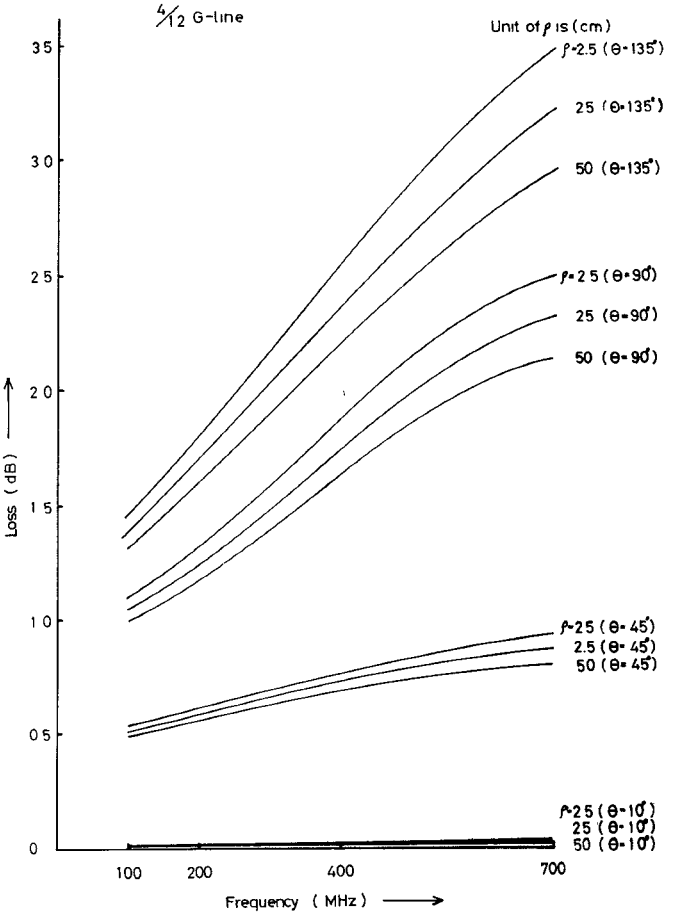

Fig. 6. Loss versus frequency.

Fig. 7, the closer an arc (distance 1_e or 1_f) gets to the center of a circle, the smaller it becomes. When the guided wave velocity v_z (viz. surface wave, an eigenvalue β) is closer to the space wave velocity c (viz. radiation wave, an eigenvalue k) the guided wave becomes a space wave.

D. Comparison with Known Theoretical Results in Some Special Cases

In Fig. 8 a comparison of our experimental results with other theoretical results is indicated. Our experimental results lie in the region between calculated values by Goubau's theory and the calculated values by Suzuki's theory.

III. Radiation from Bends and Horn

A. Radiation from Bends

Bending points do not radiate uniformly in all directions in space; the horizontal field component (E_h) is relatively large compared to the other components of the radiation field.

The maximum field strength $E_{h\max}$ (the absolute value of $E_{h\max}$ differs according to the conditions θ, f, and ρ) occurs in normalized field strengths, and is given by

$$\mathrm{dB} = -20 \log_{10} \frac{E_h}{E_{h\max}}. \tag{2}$$

The condition of measurements is shown in Table I.

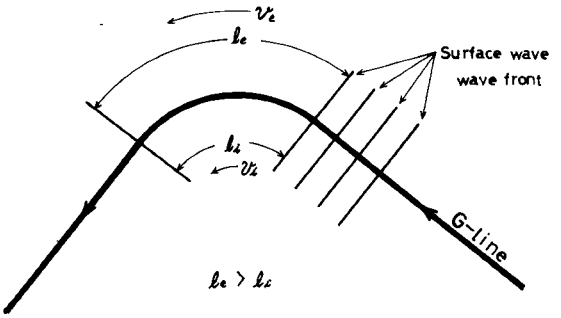

Fig. 7. Wavefront velocity in bending section.

TABLE I
Conditions of Experiment

Bending angle θ	10°	45°	90°	135°
Radius of curvature ρ	2.5 (cm)	2.5 (cm)	2.5 (cm)	2.5 (cm)
	2.5	2.5	2.5	2.5
	50	50	50	50
Frequency f (radius of circle of measurement r)	200 (MHz) [15 (m)]	200 (MHz) [15 (m)]	200 (MHz) [15 (m)]	200 (MHz) [15 (m)]
	400 (MHz) [7.5 (m)]	400 (MHz) [7.5 (m)]	400 (MHz) [7.5 (m)]	400 (MHz) [7.5 (m)]
	700 (MHz) [4.5 (m)]	700 (MHz) [4.5 (m)]	700 (MHz) [4.5 (m)]	700 (MHz) [4.5 (m)]

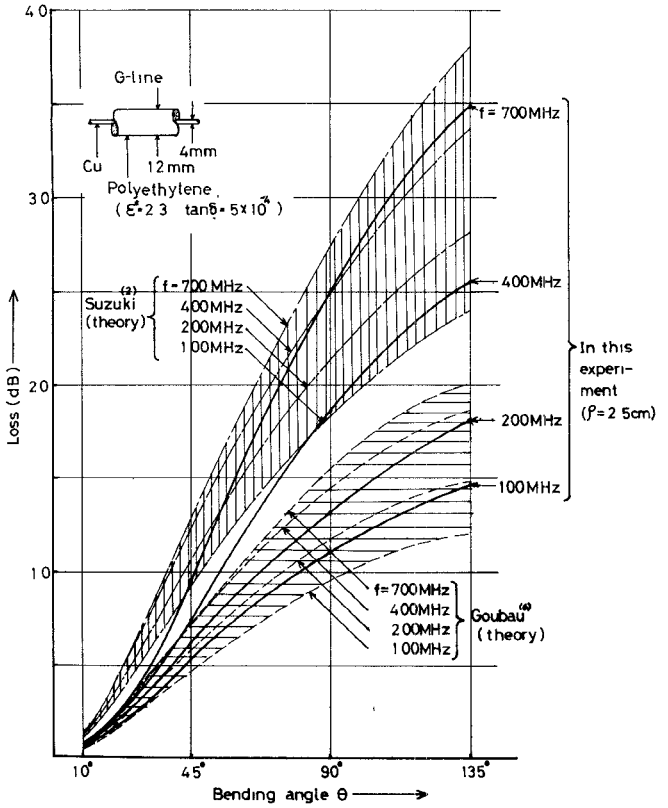

Fig. 8. The comparison between experimental results and known theoretical results.

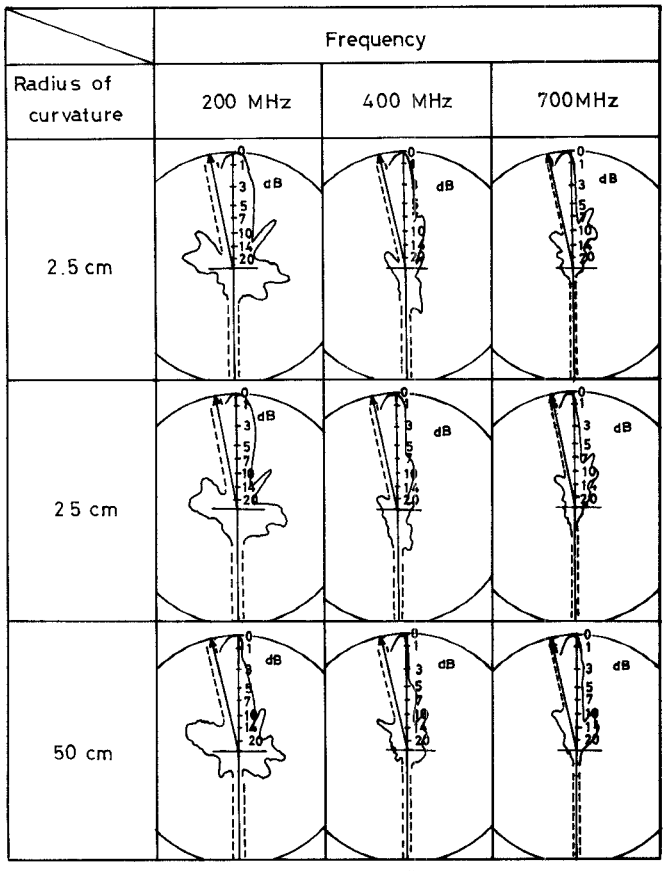

$$dB = -20 \log_{10} \frac{E_h}{E_{hmax}}$$

E_h: Horizontal electric field strength in the horizontal plane which contain G-line.

E_{hmax}: Maximum value of the E_h.

Fig. 9. Bending angle 10°.

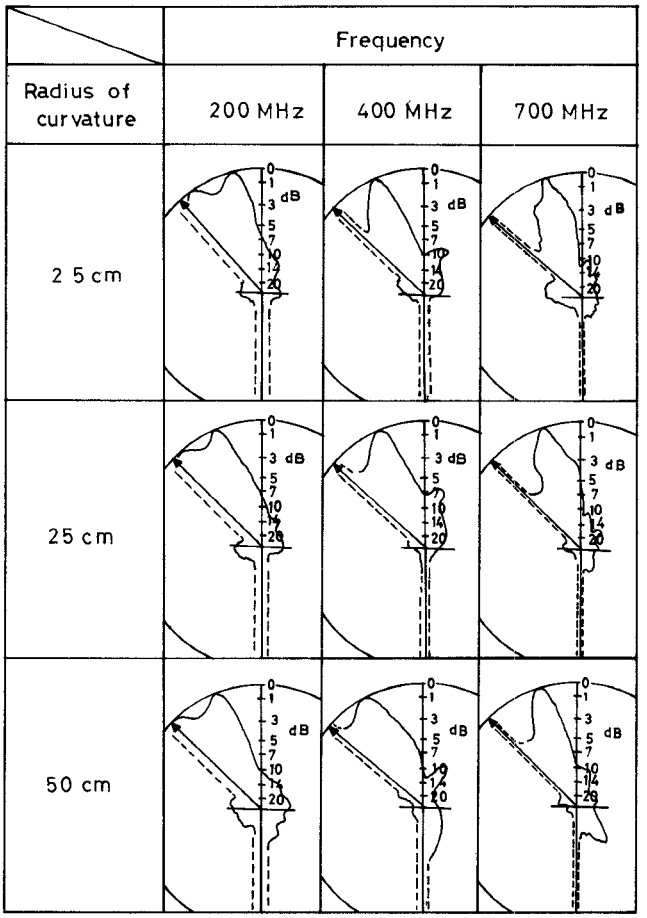

$$dB = -20 \log_{10} \frac{E_h}{E_{hmax}}$$

E_h: Horizontal electric field strength in the horizontal plane which contain G-line

E_{hmax}: Maximum value of the E_h.

Fig. 10. Bending angle 45°.

The experimental results which were obtained in the way described previously are shown in Figs. 9–12. The experimental results may be summarized as follows.

1) The change of radiation pattern with ρ is relatively small compared to the change of radiation pattern with θ.

2) When the bending angle is less than 90°, the main lobe is relatively narrow, but at angles greater than 90°, the main lobe becomes increasingly wider.

3) When the bending angle is less than 90°, the slope of the main lobe (the angle between the direction of the main lobe and the straight G-line section before the bend) gradually increases with the angle of bend.

Influence of the Radiation from the Horn: The angles between the G line and the radiation lobes at the horn are 10° at the very least (Section III-B, Figs. 13 and 14). The two radiation lobes have 20° included angles at the very least, and there is no radiation wave in the direction of the G line itself, but when we measure the radiation field due to the bend the measurement point leaves (10 wavelength) the G line, there is a weak radiation field (from the horns) and some consideration is needed before this can be overcome.

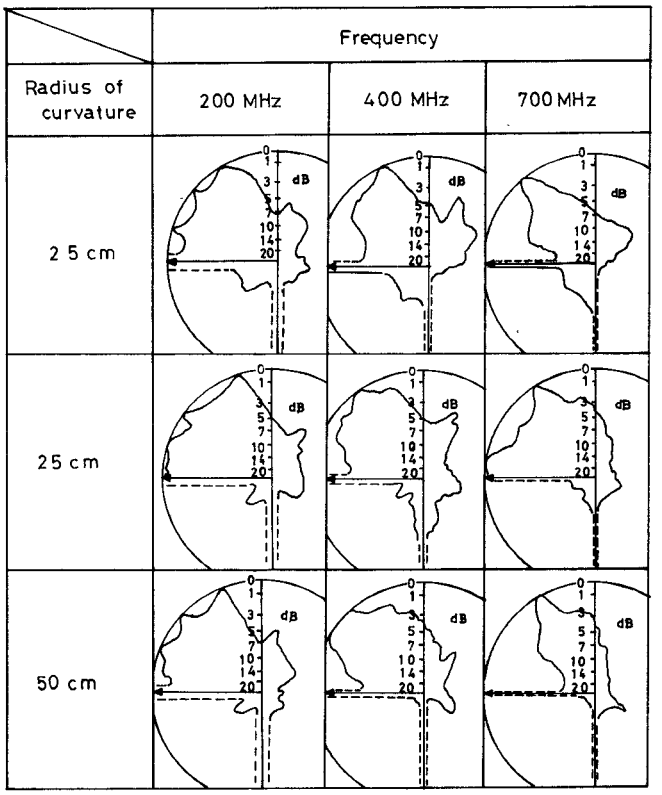

$$dB = -20 \log_{10} \frac{E_h}{E_{h\max}}$$

E_h: Horizontal electric field strength in the horizontal plane which contain G-line.

$E_{h\max}$: Maximum value of the E_h.

Fig. 11. Bending angle 90°.

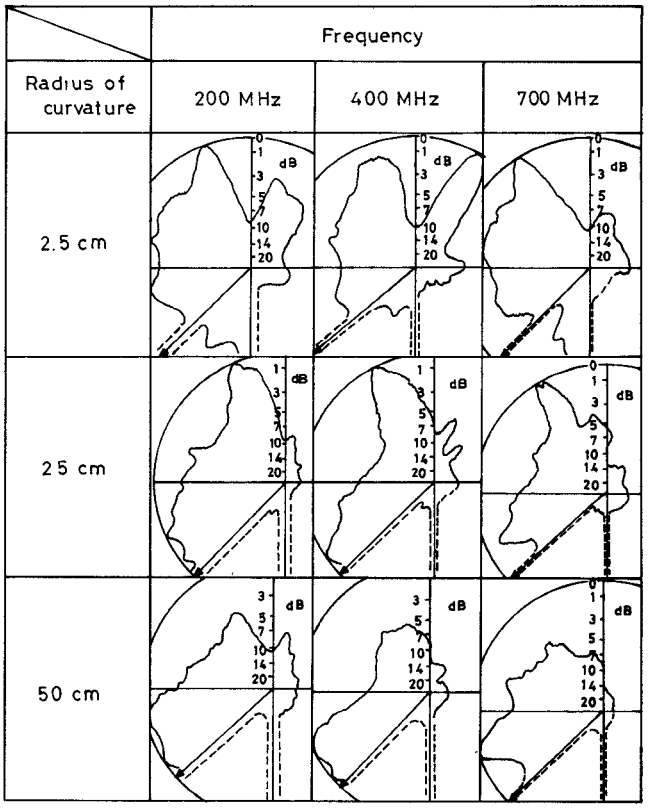

$$dB = -20 \log_{10} \frac{E_h}{E_{h\max}}$$

E_h: Horizontal electric field strength in the horizontal plane which contain G-line.

$E_{h\max}$: Maximum value of the E_h.

Fig. 12. Bending angle 135°.

If we assume that the horns are sufficiently large, radiation from the horns is not great. So we extended the horns by 1 m (axial length). In making radiation pattern measurements, it is best to employ a small receiving antenna with a corner reflector attached. The results of the experiment on the effect of radiation from the horns on the radiation pattern of the bend depended on the position; the error due to this radiation from the horns is at most 5 percent.

The experimental result of the radiation pattern, which was obtained in the aforementioned manner, is a synthetic radiation field. This radiation pattern was synthesized from elementary radiation due to the distributed radiation source current on the transmission line. The current distributions were obtained but are omitted from this paper.

B. The Radiation Patterns of the Horn

The pattern of radiation from a launching horn (Figs. 1 and 2) was measured at frequencies of 470 and 900 MHz. The results are plotted as the solid curves in Figs. 13 and 14. Also in Figs. 13 and 14, the dashed lines show the electric field of the G line itself.

The error due to radiation from the bend and the receiving horn can be negligible. (Make a high-loss transmission line by winding carbon tape around the G line; the transmission power decreases from a value of $p = 0.1$ W for the sending horn to a "negligible small value" for the bending section.)

In the case of equal transmission frequency and equal transmission power, the maximum radiation field strength $E'_{h\max}$ is about 20 dB less as compared to the $E_{h\max}$ (in the case of radiation due to bend).

IV. Conclusion

Although the surface-wave transmission line itself has a good field concentration, major radiation does occur at bends and at the horn.

This radiated field is different from the field of the surface-wave transmission line itself, and propagates some distance from the surface-wave transmission line system with a low rate of attenuation. It is important to decrease radiation from the horns and bends in order to improve transmission efficiency and quality.

On the other hand, since the pattern of radiation from a bend varies with the angle of the bend, the application of bends as radiators with feeder seems to be the most probable, for example, the community antenna and television system for houses along an ever-bending mountain stream, etc.

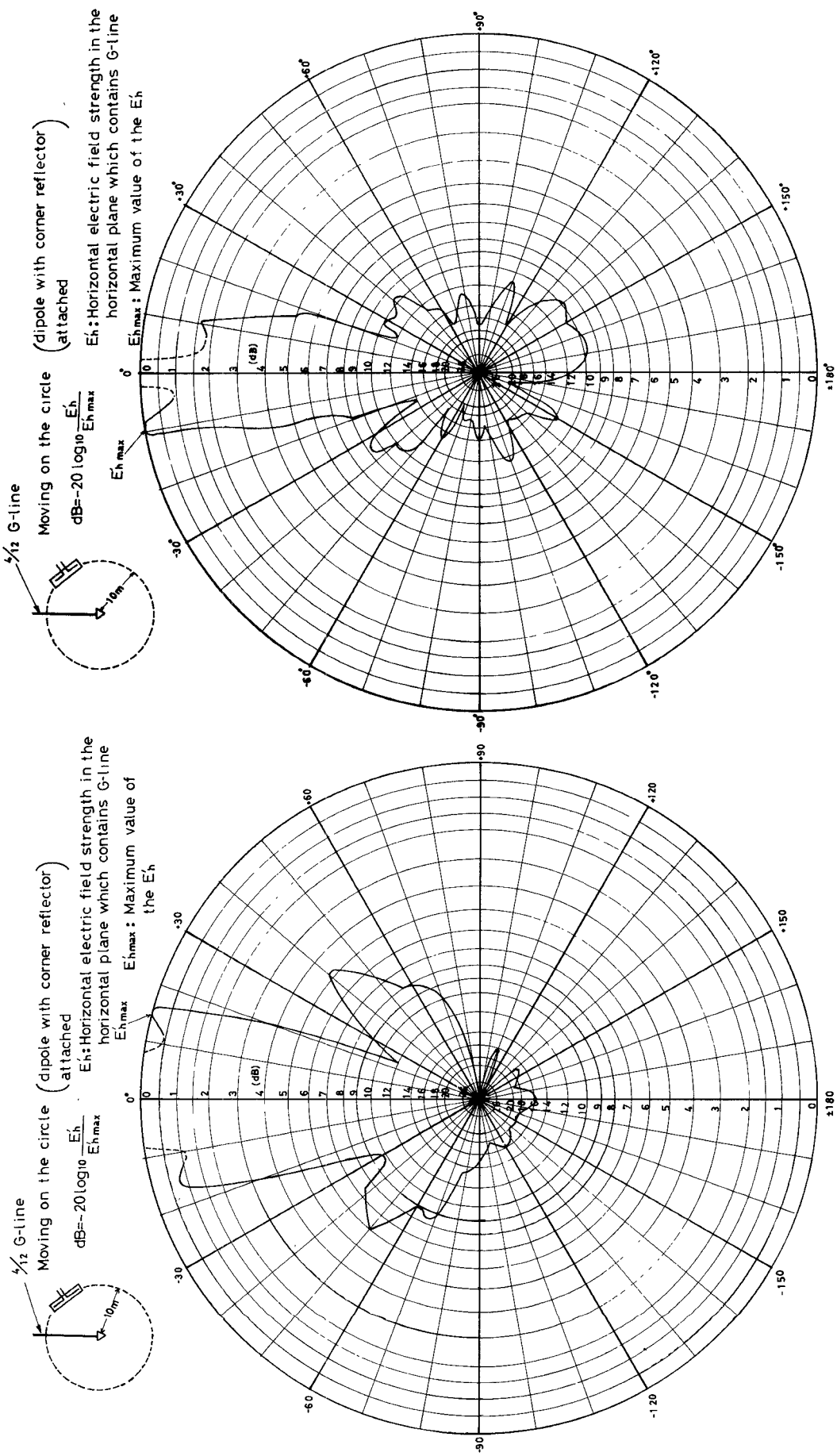

Fig. 13. Experimental patterns for 470 MHz.

Fig. 14. Experimental patterns for 900 MHz.

ACKNOWLEDGMENT

The author wishes to thank Dr. R. Sato and Dr. T. Nimura for their helpful discussions and suggestions. He also wishes to thank T. Obata, K. Fukase, T. Yaginuma, and H. Ogushi for their cooperation in the experimental work.

REFERENCES

[1] M. Takiyama, "Four-terminal network method for the bend section of a surface-wave transmission line," *Trans. of Joint Convention of the Four Electrical Institutes*, Japan, 1953.
[2] M. Suzuki, "Losses due to bending in surface-wave transmission line," *J. IECE Japan*, vol. 37, p. 33, Jan. 1954.
[3] T. Suzuki and M. Inezu, "Surface-wave transmission line experiments of 100 MHz," *Trans. of Joint Convention of the Four Electrical Institutes*, 620, 1955.
[4] Y. Moriwaki and T. Kawamura, "Loss measurements of surface-wave transmission line with electrical power meter," *Trans. of Joint Convention of the Four Electrical Institutes*, 619, 1955.
[5] E. Yasaku, "Investigation of branch-off sections of surface-wave transmission line," *Trans. of Joint Convention of the Four Electrical Institutes*, 618, 1955.
[6] G. Goubau and C. E. Sharp, "Investigations with a model surface-wave transmission line," *IRE Trans. Antennas Propagat.*, p. 222, Apr. 1955.
[7] E. Uchida and M. Nishida, "Surface-wave transmission of microwaves," presented at the Symposium of 1957 National Convention of IECE, Japan.

New Edge-Guided Mode Isolator Using Ferromagnetic Resonance Absorption

TSUTOMU NOGUCHI

Abstract—**A new edge-guided (EG) mode isolator is described in which nonreciprocal attenuation is due to the ferromagnetic resonance absorption caused by a strong dc magnetic field applied locally at the short-circuited edge of a ferrite microstrip line.**

From modal analysis, including the magnetic losses of ferrite substrate and the transversal variation of the internal dc magnetic field, the dominant EG mode has been proved to propagate along not only the conventional ferrite stripline but also a stripline with one edge short circuited to the ground. Dispersion relations and RF electric field distribution have been calculated numerically, and the upper limit of isolator bandwidth has been discussed with several design parameters. Based on the results, a practical EG mode resonance isolator has been successfully developed, which has more than 25 dB isolation loss and less than 1.0 dB insertion loss over a 4.0–8.0-GHz frequency band throughout the −10°C–+60°C temperature range.

I. INTRODUCTION

THE edge-guided (EG) mode isolator, utilizing the nonreciprocal field displacement effect in a ferrite stripline, was first investigated by Hines [1]. He constructed an isolator in which the resistive element is loaded asymmetrically on one side of the ferrite microstrip line. The isolator has very wide-band characteristics and an advantageous adaptability to MIC's. Since then, several authors have discussed the EG mode devices [2], [3]. Courtois *et al.* have used an unsaturated portion of the ferrite substrate as a reverse-wave absorber [4].

Lately, Araki *et al.* [5], [6] presented an EG mode isolator in which an edge of the ferrite microstrip is short circuited to the ground. It has a simple structure without lossy materials, a large isolation of about 60 dB, and the bandwidth of about 1–2 GHz. The operation of this isolator has been explained, via mode transformation theory, at the shorted edge discontinuity.

A new EG mode isolator was reported that used ferromagnetic resonance absorption in ferrite substrate [7]. A dc magnetic field is applied almost uniformly on the ferrite substrate by an electromagnet and is strengthened locally by a thin iron plate placed parallel to the dc field just above an edge of the strip conductor. A forward wave travels without attenuation along the edge where the field is weak. However, a backward wave, which travels along another edge where the field is strong, suffers an attenuation due to the ferromagnetic resonance absorption. The isolator performance is shown with solid lines A in Fig. 1. A fairly wide-band characteristic over 4–7 GHz is obtained.

Another simple method for obtaining an inhomogeneous internal dc field was also described [7]. This method used a disuniform demagnetizing field at the edge of the ferrite substrate with uniform field application. Even if a uniform field is applied, the internal dc magnetic field increases steeply at the edge of the ferrite substrate, because of the spontaneously induced disuniform demagnetizing field [8]. In fact, it has been proved experimentally [7] that nonreciprocal transmission losses are obtained when the center conductor has gotten near to the edge of the ferrite.

In further experiments [9], a strong local field was applied along short-circuited edge of the stripline which was proposed by Araki *et al.*, as shown in Fig. 2. In this case, the center conductor will be called a short–open boundary

Manuscript received February 19, 1976; revised July 28, 1976.
The author is with the Electron Device Research Laboratory, Central Research Laboratories, Nippon Electric Company Ltd., Kawasaki, Japan.